Probabilistic Seismic Hazard Analysis Using Stochastic Simulated Ground Motions

Sarah Azar
PhD Student, Dept. of Civil and Environmental Engineering, American University of Beirut, Lebanon

Mayssa Dabaghi
Assistant Professor, Dept. of Civil and Environmental Engineering, American University of Beirut, Lebanon

Sanaz Rezaeian
Research Structural Engineer, United States Geological Survey (USGS), Golden CO, USA

ABSTRACT: In recent years, ground motion models used in probabilistic seismic hazard analyses have evolved from the traditional approach of using ground motion prediction equations (GMPEs) to using ground motion time series models. The purpose of this paper is to develop an approach to perform a probabilistic seismic hazard analysis using stochastic site-based simulation techniques. These techniques consist of empirical stochastic models that simulate both near-fault and far-field ground motion time series. The near-fault models consider directivity pulses, which can impose large seismic demands. The proposed approach was applied to a site located in downtown Los Angeles, California, and the corresponding hazard curves were developed. The results were compared to hazard curves derived for the same site from CyberShake, which uses a physics-based simulation approach, and from a traditional GMPE approach. The comparison indicated that the proposed methodology accurately describes the seismic hazard at the site at high hazard levels. The proposed approach is computationally efficient compared to the use of physics-based simulations like CyberShake.

1. INTRODUCTION

Probabilistic seismic hazard analysis (PSHA) is a commonly used method for evaluating the rate of exceeding a ground motion level at a site of interest in a certain time interval. A PSHA framework involves a seismic source model combined with a ground motion model. The seismic source model defines the rupture scenarios that may affect the site of interest while the ground motion model defines the expected distribution of the ground motion levels due to the possible earthquake scenarios. In the context of PSHA, there are two types of ground motion models: empirical ground motion prediction equations (GMPEs) and ground motion time series models, which can be either deterministic physics-based or stochastic models. Traditional PSHA employs GMPEs. Implementing these models in a probabilistic framework is based on the ergodic assumption, which may result in an overestimation of the hazard level over long return periods (Anderson and Brune 1999).

In recent years, PSHA has progressed from the conventional analysis of using GMPEs to using models of ground motion time series. Characterization of the probability distribution of the ground motion level in terms of synthetic time series rather than GMPEs is desirable for several reasons. For instance, the ground motions that contribute the most to hazard often drive structures into the non-linear range. In that case, a non-linear response-history analysis using time series is necessary. Moreover, GMPEs (e.g. Abrahamson et al. 2014) do not consider most local effects such as the seismic demands imposed by near-fault ground motions. In fact, such

motions are likely to contain pulses mainly due to directivity effects and consequently impose larger demands on structures (e.g. Makris and Black 2004) .

Several ground motion time series simulation techniques have been proposed in PSHA. Most have utilized deterministic physics-based techniques that are source based and explicitly model the physical process of the seismic source to evaluate the propagation of seismic waves and determine the site response (e.g. Moczo et al. 2007). Graves et al. (2011) presented a source-based computational approach to PSHA as part of a Southern California Earthquake Center (SCEC) research project. The proposed model, called CyberShake, uses Version 2.0 of the Uniform California Earthquake Rupture Forecast (UCERF 2.0) as the source characterization model (Field et al. 2009). CyberShake then generates synthetic seismograms using seismic reciprocity for a set of rupture variations. Due to computational limitations, generated ground motions are limited to frequencies less than 1 Hz depending on the spatial resolution of the fault rupture model (Graves et al. 2011). In more recent studies, the CyberShake hazard model is planned to be extended to higher frequencies by combining the 1 Hz physics-based synthetics with high-frequency stochastic motions (SCECpedia 2018). Implementing physics-based simulations in hazard analyses has a number of advantages as these models can represent the local wave propagation effects. Through the use of a 3D velocity model, amplification of the ground motion in sites susceptible to forward directivity and basin effects is naturally taken into account. However, generating a large number of synthetic ground motions using this model is computationally consuming.

Alternatively, broadband site-based stochastic models can be used to generate synthetic ground motions. These models use a stochastic process to describe the ground motion time series as it is observed at a site. Rezaeian and Der Kiureghian (2010; 2012) developed a parameterized stochastic model for the simulation of far-field ground motions. For near-fault ground motions, Dabaghi and Der Kiureghian (2017; 2018) proposed a simulation procedure that generates pulse-like and non-pulse-like ground motions in appropriate proportions. Both models employ a modulated and filtered white-noise process with time-varying filter parameters and are able to account for the natural variability in the ground motions. Stochastic simulation models are computationally efficient and have more practical formulations compared to other types of simulation techniques. Such models can generate multiple realizations of a given scenario using few input parameters easily accessible to engineers. Site-based models implicitly account for the effect of source, path and site conditions through the model parameters.

Several attempts have been made to implement site-based models in a PSHA framework. Dabaghi et al. (2013) illustrated a similar approach using an earlier version of their simulation model. The seismic source considered was a simple fault located near the site. This study emphasized the importance of accounting for both pulse-like and non-pulse-like ground motions in a PSHA approach. A few other attempts have been made to improve the implementation of site-based stochastic models in a PSHA framework (e.g. Yamamoto 2011). However, these attempts failed to consider an accurate source characterization. For a reliable estimation of the seismic hazard at a site, a more realistic source model should be considered, and both near-fault and far-field synthetic ground motions should be included.

This paper describes an approach for performing PSHA using site-based stochastic simulation techniques. The methodology is similar to the approach previously developed by Dabaghi et al. (2013). However, it builds on it by using the most up-to-date version of the ground motion models (Dabaghi and Der Kiureghian 2018; Rezaeian and Der Kiureghian 2012), as well as more realistic earthquake scenarios. The developed approach is applied to a site located in downtown Los Angeles, California. The resulting hazard curves are then compared to the outputs of

CyberShake and conventional GMPEs at the same site. The proposed approach can contribute to performance-based earthquake engineering by providing a probabilistic framework that is reliable, practical and computationally efficient.

2. SIMULATION-BASED PSHA METHODOLOGY

This paper uses a stochastic site-based model to perform PSHA. The first step involves source characterization, which consists of identifying all earthquake ruptures that may occur at a given location and their corresponding rates of occurrence. Monte Carlo simulations are then used to develop a number of earthquake catalogs for a selected period of study. Each catalog represents possible earthquake scenarios that may occur at the site of interest over the period of study. For each scenario included in the catalog, a synthetic ground motion time series is generated. The set of simulated ground motions is then used to produce pseudo-spectral acceleration hazard curves at various periods.

2.1. Seismic Source Model

A seismic source model describes the geometry and magnitude of possible earthquake ruptures and their associated probabilities of occurrence over a specified time. As mentioned earlier, the seismic source model used in the proposed framework is based on UCERF 2.0 (Field et al. 2009). In particular, this paper uses the latest earthquake rupture forecast used in the CyberShake framework at the time of the study, namely ERF36, which is characterized by a 200-m rupture surface resolution. Using the same source model allows evaluating the effect of the ground motion model on PSHA results. The modifications and additional constraints applied by CyberShake on UCERF 2.0 are thus also applied in this study. These alterations include setting the minimum magnitude of considered earthquakes to 6, excluding background seismicity, and adjusting rupture areas for consistency with the simulation model (Graves et al. 2011). For a specific site, only ruptures within 200 km of the site are considered in the hazard calculation. These ruptures are assumed to follow independent Poisson distributions with annual probabilities of occurrence provided in CyberShake. For each rupture, CyberShake then introduces a suite of variations in the hypocenter location and slip distribution, thus accounting for the natural variability in the ground motions. This process results in an average of 415,000 scenarios for each site. The rupture variation generator used is based on a hybrid broadband ground-motion simulation methodology (Graves and Pitarka 2015).

For the simulation-based PSHA approach proposed in this study, the source model is defined in terms of the magnitude, location, and geometry of relevant ruptures, their annual probability of occurrence, and the variation in hypocenter locations for each rupture. This source information is sufficient to obtain the input necessary for the simulation model used in this study (information about slip distributions is not required).

2.2. Stochastic Earthquake Catalog

After extracting all the I possible earthquake ruptures that may affect the site of interest and their associated annual Poisson probabilities P_i, $i = 1 \dots I$, we use the Monte Carlo method to generate any number of synthetic earthquake catalogs over a period of Y years.

Given the set of ruptures $i = 1 \dots I$ that can affect the site, their associated annual probabilities P_i, and the number of rupture variations k_i (number of variations in the hypocenter location), a stochastic ground motion catalog is generated as follows. First, the mean annual rupture rate λ_i is calculated by assuming that the number of earthquakes from rupture i follows a Poisson distribution:

$$\lambda_i = -log(1 - P_i) \quad (1)$$

Secondly, a random number is simulated from a Poisson distribution with a mean rate equal to $\lambda_i \times Y$. It represents the number of occurrences N_i of the ith rupture in the next Y years. Next, for each of these occurrences $n_i = 1 \dots N_i$, a random number is drawn from a uniform distribution

ranging from 1 to k_i. This number represents the rupture variation (hypocenter location) to be considered. These steps result in N_i different earthquake scenarios caused by the i^{th} rupture. The same procedure is applied to all the identified ruptures. The simulated catalog then consists of the collection of the $\sum_i N_i$ selected earthquake scenarios, which affect the considered site in Y years. This procedure can be repeated multiple times to generate any number of synthetic earthquake catalogs. These catalogs are considered as possible realizations of the sets of earthquake events that may affect the site over a duration of Y years.

2.3. Simulated Stochastic Ground Motions

For each earthquake scenario in the synthetic catalog, a ground motion is simulated using the stochastic site-based model. This model requires the definition of an earthquake scenario to include the moment magnitude (M_w), the type of faulting F ($= 0$ for strike-slip faults, $= 1$ otherwise), the closest distance R_{rup} from the site to the fault rupture plane, and the 30-m averaged soil shear-wave velocity V_{s30} at the site. The near-fault model requires the depth Z_{TOR} to the top of the fault rupture and directivity parameters $s_{or}d$ and $\theta_{or}\phi$ as additional input parameters (Somerville et al. 1997). For strike-slip faulting, the parameter s represents the length of the fault rupturing between the epicenter and the site. The parameter θ is defined as the angle in the horizontal plane between the fault plane and the direction between the epicenter and the site. For dip-slip faulting, the directivity parameter d represents the width of the fault rupturing between the hypocenter and the site. The parameter ϕ denotes the angle in a vertical plane between the fault plane and the direction between the hypocenter and the site. In summary, each earthquake scenario must be defined in terms of the input parameters (F, M_w, Z_{TOR}, R_{rup}, V_{s30}, $s_{or}d$, $\theta_{or}\phi$).

The CyberShake database provides the coordinates and V_{s30} values for several sites. For any rupture i affecting a site of interest, M_w, rupture geometry (strike, dip, and coordinates of the points defining the rupture plane), and rake angle are extracted from the CyberShake database for the earthquake rupture forecast used (ERF36). The values of Z_{TOR} are calculated based on the rupture geometry while the values of F are inferred from the rake angle. Then, given the coordinates of the site, R_{rup} is calculated. Next, with the hypocenter coordinates corresponding to rupture variation k_i, which are also obtained from CyberShake, $s_{or}d$ and $\theta_{or}\phi$ are calculated.

After determining the corresponding parameters, a synthetic ground motion time series is simulated for each scenario in each catalog. The far-field stochastic model is used for scenarios where $R_{rup} > 30$ km. For smaller distances, the near-fault stochastic model is more appropriate since it accounts for possible directivity effects. This near-fault model integrates a probability model that predicts the likelihood of observing a directivity pulse at a near-fault site (Shahi and Baker 2014). This allows the generation of both pulse-like and non-pulse-like motions in reasonable proportions.

For each synthetic earthquake catalog, the end result is a set of synthetic ground motion time series corresponding to the earthquake scenarios of the catalog. Each set is considered as one realization of the possible ground motions that may affect the site of interest in Y years.

2.4. Hazard Curves

The primary outputs of a PSHA are seismic hazard curves. These curves plot the estimated annual rate or probability of exceedance of ground motion intensity measures. The most common intensity measure is the pseudo-spectral acceleration $S_a(T)$ at a specified period of interest. To develop such hazard curves, the value of $S_a(T)$ is first computed for each simulated time series in a Y-year catalog. The mean annual rate of exceedance $\lambda_{(\alpha)}$ of one intensity threshold α is then calculated as follows:

$$\lambda_{(\alpha)} = R_{(\alpha)}/Y \qquad (2)$$

where $R_{(\alpha)}$ is the total number of ground motions for which $S_a(T) > \alpha$ during the Y-year period. Equation 2 is applied in this study because the

earthquake catalog is simulated using the Monte Carlo method. Similarly, the annual rate of exceedance of other response thresholds at period T are calculated. Lastly, for each synthetic catalog, hazard curves at the site are generated in terms of $S_a(T)$ by plotting the mean annual rate of exceedance of the corresponding response thresholds.

3. CASE STUDY: LOS ANGELES, CALIF.

The proposed approach is illustrated on a site selected from the CyberShake platform and located in downtown Los Angeles (LADT). The LADT site has a latitude of 34.05204, a longitude of -118.25713 and a V_{s30} of 390 m/s. The relevant seismic ruptures and their annual rates of occurrence ($\lambda_i's$) are extracted from the CyberShake database. These seismic ruptures are used to define the set of all possible earthquake scenarios affecting the LADT site. A total of $I = 7019$ seismic ruptures are extracted and 476,920 corresponding earthquake scenarios are identified. The scenarios have M_w ranging between 6 and 8.25 and R_{rup} ranging from 4 to 200 km. The earthquake scenarios are then used in Monte Carlo simulations to generate 10 synthetic earthquake catalogs for LADT, each over a period of 10,000 years. Each catalog contains a different set of scenarios that might affect the site.

Table 1: Total number of earthquakes/ground motions (Nb of GMs) in each Monte Carlo (MC) simulated catalog

MC	*1*	*2*	*3*	*4*	*5*
Nb of GMs	*1067*	*1048*	*1057*	*1027*	*1039*
MC	*6*	*7*	*8*	*9*	*10*
Nb of GMs	*977*	*1062*	*1080*	*1037*	*1012*

Table 1 lists the number of earthquake scenarios in each LADT catalog. The average of 1041 earthquakes per catalog implies a mean annual rate of earthquake occurrence equal to 0.1041 and is consistent with the sum of the annual rates of occurrence of the relevant ruptures provided by CyberShake, $\sum_{i=1}^{I} \lambda_i = 0.1041$. Finally, as described in Section 2.3, the stochastic model is used to simulate a synthetic ground motion time series for each scenario in each catalog.

3.1. Hazard Curves

For each simulated ground motion time series, $RotD50\ S_a(T)$ is computed at various periods and at a fixed viscous damping ratio of 5% (Boore 2010). For each Monte Carlo simulation, hazard curves of $RotD50\ S_a(T)$ are then calculated as described in Section 2.4. These hazard curves are compared with hazard curves from CyberShake, computed by SCEC at the same site, and with hazard curves from the NGA-West2 GMPEs, generated using the OpenSHA application (Field et al. 2003). The same seismic source model (UCERF 2.0) is used in the three methodologies; the only difference is the ground motion models.

Figure 1 compares the RotD50 $S_a(T)$ hazard curves from the proposed simulation-based PSHA with the corresponding hazard curves derived from CyberShake and from the NGA-West2 GMPEs at periods of 0.1s, 0.2s, 0.5s, 1s, 2s, and 5s. The CyberShake study from which the hazard curves are extracted uses a physics-based model for frequencies lower than 1 Hz in combination with broadband components for higher frequencies, and in its current version is known to be accurate only up to 2 Hz. The GMPEs curve corresponds to a weighted average of the five NGA-West2 GMPEs (Rezaeian et al. 2014). The plots also specify the commonly used hazard levels corresponding to a 2%, 5% and 10% probability of exceedance in 50 years.

Since the same source model is used for the different hazard curves, the annual rate of occurrence of an earthquake at the site should be consistent. This is illustrated in Figure 1 where the rates of exceedance at low $S_a(T)$ thresholds are the same for all hazard curves. The differences observed at higher hazard levels are due to the ground motion models used to develop these curves. As can be observed in Figure 1, at periods less than 0.5s and at high hazard levels, the CyberShake results are lower than the results of our simulation-based PSHA. However, as the period increases, our hazard curves approach those resulting from CyberShake with the latter

slightly exceeding the former at low hazard levels. As mentioned earlier, at frequencies <1 Hz, the CyberShake results are based on physics-based models that account for basin effects. Since the results from both approaches are similar in this frequency range, the proposed methodology is considered to be accurate at long periods.

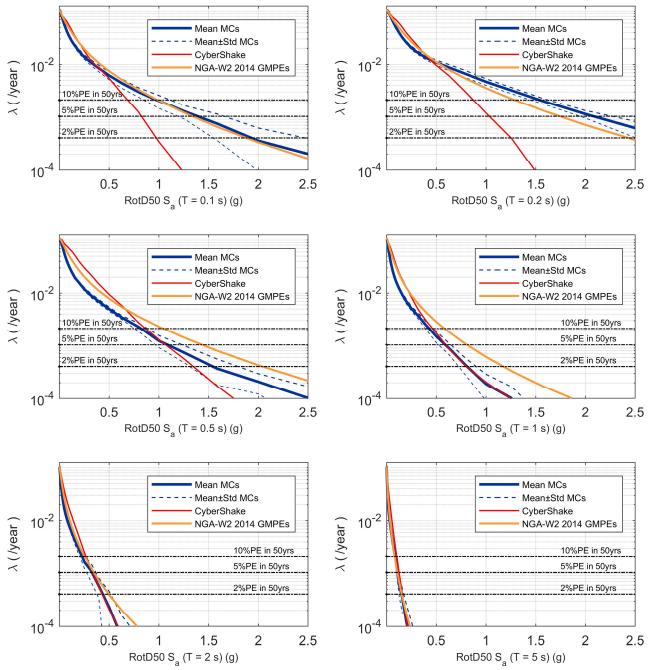

Figure 1: RotD50 $S_a(T)$ hazard curves from the proposed simulation-based PSHA compared with CyberShake and NGA-West2 GMPEs hazard curves at the LADT site at different periods and for a damping ratio of 5%.

On the other hand, Figure 1 shows that the results from our simulation-based PSHA at short periods (0.1s and 0.2s) are quite similar to those derived from the NGA-West2 GMPEs. These GMPEs are known to be more accurate than physics-based simulations at higher frequencies. This confirms that our site-based simulations are more adequate than the simulations used in CyberShake in representing the high frequency content. Figure 1 also shows some differences in the hazard curves at T=0.5s and T=2s between the simulation-based PSHA and GMPEs hazard curves. To further interpret these differences, a disaggregation at the specified hazard levels is needed to determine the scenarios that are contributing most to the hazard at those levels. For these scenarios, the ground motion levels predicted by the site-based model and the GMPEs should be compared. This analysis is discussed in the next section.

3.2. Disaggregation

Disaggregation of the hazard curves at LADT was applied to the simulated ground motion catalog with $Y = 100{,}000$ years. This catalog is obtained by combining the ten 10,000-years catalogs. Figure 2 shows the magnitude/distance disaggregation of the 0.2s and 1s RotD50 $S_a(T)$ hazard curves for a 5% probability of exceedance in 50 years from both the proposed methodology and the NGA-West2 GMPEs.

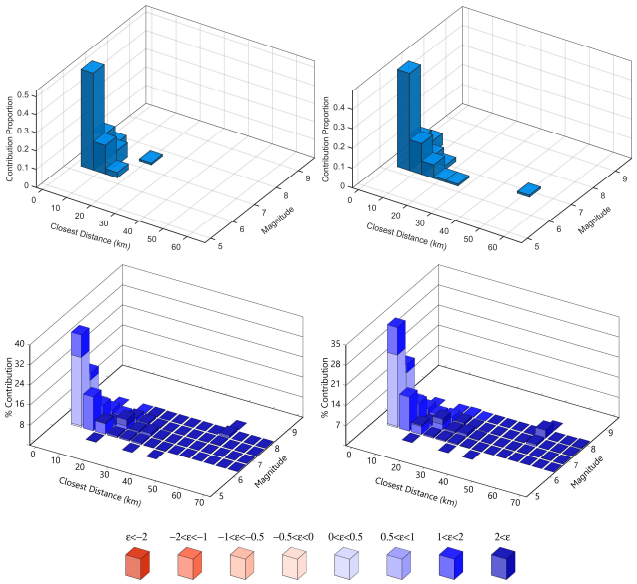

Figure 2: Magnitude/Distance disaggregation at LADT for 0.2s and 1s RotD50 $S_a(T)$ at 5% probability of exceedance in 50 years. Top panel is based on the proposed simulation-based PSHA and bottom panel is derived from the NGA-West2 GMPEs.

For simulation-based PSHA, the seismic hazard level at $T = 0.2$ s and 1 s is controlled by earthquakes ruptures with magnitudes ranging from 6.25 to 6.75 and distances ranging from 2.5 to 7.5 km. This disaggregation pattern is also observed at the other periods and hazard levels considered. As shown in Figure 2, the pattern is generally consistent with the GMPEs results, which validates the proposed methodology. However, the proposed approach shows a higher

contribution from nearby sources as opposed to the conventional GMPE approach, where distant sources with large epsilon (ϵ) values contribute in low proportions to the high hazard levels.

To explain the differences in the hazard curves between the two approaches, the ground motion levels estimated by the two ground motion models for the most contributing scenario are compared. Based on the previous analysis, this scenario has the following parameters: $M_w = 6.5$, $R_{rup} = 5$ km and $V_{s3} = 390$ m/s. Multiple synthetic motions are generated using the near-fault model for the same M_w, R_{rup} and V_{s30} values but by using different hypocenter-site combinations. This provides a proper representation of the possible directivity conditions for the given scenario. In Figure 3, the statistics of the 5% damped RotD50 $S_a(T)$ response spectra of the resulting motions are compared with those of the weighted NGA-West2 GMPEs for the same scenario (with $F = 0$).

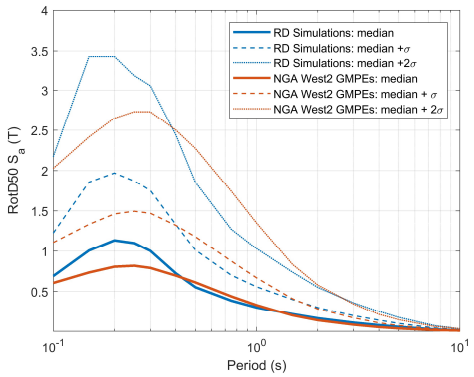

Figure 3: 5% damped RotD50 $S_a(T)$ response spectra from 600 random-directivity synthetic motions and from the weighted average of the NGA-West2 GMPEs for the scenario: $F = 0$, $M_w = 6.5$, $R_{rup} = 5$ km and $V_{s30} = 390$ m/s.

Since the GMPE disaggregation shows significant contribution for $\epsilon > 0.5$ as shown in Figure 2, the analysis of the results should be based on these ground motion levels. For example, at the median plus one standard deviation level, the $S_a(T)$ values from the simulations are slightly larger than the GMPEs values at $T = 0.1$ s and at $T = 0.2$ s, where the difference is more pronounced. The observed pattern is consistent with the difference observed in Figure 1 at these periods. A similar analysis at the other periods can explain the GMPEs higher rates at $T = 0.5$ s and 1 s and the similar results observed at the longer periods.

The characteristics of the contributing ground motions at the 5% in 50 years hazard level are also identified. Since the stochastic model implemented in the proposed methodology considers directivity effects, some of these contributing ground motions are pulse-like motions. Table 2 represents their proportion as well as their mean pulse period $\overline{T_p}$ .The table shows that as the period of the oscillator increases, the number of contributing pulse-like ground motions increases up to periods of 1-2 s then decreases for longer periods. The table also indicates that $\overline{T_p}$ tends toward the oscillator's period for $T \geq 1$ s. When the oscillator is subjected to ground motions with a predominant period close to its natural period, the response of the SDOF is amplified. These pulse-like ground motions hence make a stronger contribution to the hazard at these periods. Note that the pulses in the simulated catalogs all have periods above 0.4 s. Thus, pulse-like motions are not expected to make a significant contribution to short-period oscillators (T=0.1-0.5 s).

Table 2: Percentage of pulse-like ground motions (GMs) of the motions contributing to the 5% probability of exceedance in 50 years hazard level and their mean pulse period $\overline{T_p}$

Period (s)	*0.1*	*0.2*	*0.5*	*1*	*2*	*5*
% pulse GMs	*14*	*18*	*42*	*66*	*66*	*35*
$\overline{T_p}$ *(s)*	*1.6*	*1.9*	*1.3*	*1.2*	*2.0*	*3.2*

4. CONCLUSIONS

This paper proposed an approach to perform PSHA using synthetic ground motions from stochastic site-based models. The approach was applied to a site located in downtown Los Angeles, California, using UCERF 2.0 as a source model. Monte Carlo simulations were then performed to generate earthquake ground motion catalogs at the site of interest over a period of 10,000 years. Synthetic ground motions were simulated using parameterized stochastic models

for far-field and near-fault ground motions. The resulting hazard curves were compared to results derived from a recent CyberShake study and from the traditional GMPE approach. The results indicated that the proposed approach describes accurately the seismic hazard at a wide range of periods and at the common hazard levels. The disaggregation at the 5% in 50 years hazard level showed that the proposed methodology shows a higher contribution from nearby sources compared to GMPEs. As expected, the disaggregation proved that the mean pulse period increases with the SDOF's natural period for $T \geq 1$ s.

The proposed approach offers a reliable tool for estimating hazard levels at a broad range of periods. Implementing stochastic site-based models in a PSHA framework is practical and does not require significant computational resources as opposed to using physics-based simulations. The latter, however, account for local basin effects as opposed to the site-based model. The framework can be extended to evaluate the dynamic response of structures when subjected to the simulated ground motion time series and can consequently contribute to the development of performance-based design in seismic engineering.

5. ACKNOWLEDGMENTS

The authors are grateful to Kevin Milner, Scott Callaghan, and Rob Graves for answering our questions about the CyberShake platform.

6. REFERENCES

Abrahamson, N. A., Silva, W. J., and Kamai, R. (2014). "Summary of the ASK14 ground motion relation for active crustal regions." *Earthquake Spectra*, 30(3), 1025-1055.

Anderson, J. G., and Brune, J. N. (1999). "Probabilistic Seismic Hazard Analysis without the Ergodic Assumption." *Seismological Research Letters*, 70(1), 19-28.

Boore, D. M. (2010). "Orientation-independent, nongeometric-mean measures of seismic intensity from two horizontal components of motion." *Bulletin of the Seismological Society of America*, 100(4), 1830-1835.

Dabaghi, M., and Der Kiureghian, A. (2017). "Stochastic model for simulation of near‐fault ground motions." *Earthquake Engineering & Structural Dynamics*, 46(6), 963-984.

Dabaghi, M., and Der Kiureghian, A. (2018). "Simulation of orthogonal horizontal components of near‐fault ground motion for specified earthquake source and site characteristics." *Earthquake Engineering & Structural Dynamics*, 47(6), 1369-1393.

Dabaghi, M., Der Kiureghian, A., Rezaeian, S., and Luco, N. "Seismic hazard analysis using simulated ground motions." *Proc., 11th International Conference on Structural Safety & Reliability*.

Field, E. H., Dawson, T. E., Felzer, K. R., Frankel, A. D., Gupta, V., Jordan, T. H., Parsons, T., Petersen, M. D., Stein, R. S., Weldon, R. J., II, and Wills, C. J. (2009). "Uniform California Earthquake Rupture Forecast, Version 2 (UCERF 2)." *Bulletin of the Seismological Society of America*, 99(4), 2053-2107.

Field, E. H., Jordan, T. H., and Cornell, C. A. (2003). "OpenSHA: A developing community-modeling environment for seismic hazard analysis." *Seismological Research Letters*, 74(4), 406-419.

Graves, R., Jordan, T. H., Callaghan, S., Deelman, E., Field, E., Juve, G., Kesselman, C., Maechling, P., Mehta, G., Milner, K., Okaya, D., Small, P., and Vahi, K. (2011). "CyberShake: A Physics-Based Seismic Hazard Model for Southern California." *Pure and Applied Geophysics*, 168(3), 367-381.

Graves, R., and Pitarka, A. (2015). "Refinements to the Graves and Pitarka (2010) Broadband Ground-Motion Simulation Method." *Seismological Research Letters*, 86(1), 75-80.

Makris, N., and Black, C. J. (2004). "Evaluation of peak ground velocity as a "good" intensity measure for near-source ground motions." *Journal of Engineering Mechanics*, 130(9), 1032-1044.

Moczo, P., Kristek, J., Galis, M., Pazak, P., and Balazovjech, M. (2007). "The finite-difference and finite-element modeling of seismic wave propagation and earthquake motion." *Acta Physica Slovaca*, 57(2).

Rezaeian, S., and Der Kiureghian, A. (2010). "Simulation of synthetic ground motions for specified earthquake and site characteristics." *Earthquake Engineering & Structural Dynamics*, n/a-n/a.

Rezaeian, S., and Der Kiureghian, A. (2012). "Simulation of orthogonal horizontal ground motion components for specified earthquake and site characteristics." *Earthquake Engineering & Structural Dynamics*, 41(2), 335-353.

Rezaeian, S., Petersen, M. D., Moschetti, M. P., Powers, P., Harmsen, S. C., and Frankel, A. D. (2014). "Implementation of NGA-West2 ground motion models in the 2014 US National Seismic Hazard Maps." *Earthquake Spectra*, 30(3), 1319-1333.

SCECpedia (2018). "CyberShake study 15.12." <https://scec.usc.edu/scecpedia/CyberShake_Study_15.12>.

Shahi, S. K., and Baker, J. W. (2014). "An Efficient Algorithm to Identify Strong-Velocity Pulses in Multicomponent Ground Motions." *Bulletin of the Seismological Society of America*, 104(5), 2456-2466.

Somerville, P. G., Smith, N. F., Graves, R. W., and Abrahamson, N. A. (1997). "Modification of empirical strong ground motion attenuation relations to include the amplitude and duration effects of rupture directivity." *Seismological Research Letters*, 68(1), 199-222.

Yamamoto, Y. (2011). "Stochastic model for earthquake ground motion using wavelet packets." Doctor of Philosophy, Stanford University.